# Direct Observation of Plasma Dielectric Motion

F. Skiff and F. Anderegg
*Centre de Recherches en Physique des Plasmas, Association EURATOM—Confédération Suisse, Ecole Polytechnique Fédérale de Lausanne, CH-1007 Lausanne, Switzerland*
(Received 31 March 1987)

Local measurement in magnetized plasma of the ion-velocity distribution function synchronous with an externally launched electrostatic wave carries information concerning the wavelength perpendicular to the magnetic field as well as the wave amplitude and phase.

PACS numbers: 52.35.−g

Dispersion relations in hot magnetized plasma are generally obtained by taking moments of the perturbed (one-body) distribution function in the presence of the self-consistent mean electromagnetic field. Although wave dispersion relations are determined by the averaged plasma response, considerable information on the wave fields is contained in the distributions. In particular, in this Letter we report the measurement of the electric field and perpendicular wave number of an electrostatic wave in magnetized plasma through local phase-locked measurements of the ion distribution function. To provide equivalent information, the averaged ion motion must be measured at several distinct positions. Coherent oscillations of the ion distribution function during electrostatic ion-cyclotron wave instability were first observed by Stern,[1] and more recently by McWilliams and Sheehan,[2] but the results were not compared to linear theory. In the experiments reported here, waves are generated with use of electrostatic antennas.

From the Vlasov equation, one readily obtains an expression for the perturbed distribution function given the equilibrium distribution function $f_0$ and the electrostatic perturbation $\mathbf{E}$,[3]

$$f^1(\mathbf{v},\mathbf{x},t)=\frac{-q}{m}\int_{-\infty}^{t}\mathbf{E}(\mathbf{X}(t'),t')\cdot\nabla_v f_0\,dt'. \tag{1}$$

Here the integral is performed along the particle orbits $(\mathbf{X}(t),\mathbf{V}(t))$, and $q/m$ is the charge-to-mass ratio of the particle species considered. Evaluating Eq. (1) for the case of uniform magnetized plasma ($B=B_0\hat{\mathbf{z}}$), Maxwellian equilibrium distribution, and integrating over the Cartesian velocity coordinates in the plane of the electric field $(v_x,v_z)$ one obtains

$$f^1(v_y,\mathbf{x},t)=\frac{-q\phi(\mathbf{x},t)}{mv_t^2}\sum_{n,m=-\infty}^{\infty}J_m(a)I_n\left(\frac{\lambda}{4}\right)e^{ia-\lambda-im\pi/2}\zeta_0 Z(\zeta_{2n+m})f_0(v_y), \tag{2}$$

where $a\equiv k_x v_y/\Omega_c$, $\lambda\equiv(k_x v_t/\Omega_c)^2$, $\zeta_n=(\omega-n\Omega_c)/(\sqrt{2}k_z v_t)$, $\Omega_c\equiv qB_0/mc$, and $v_t$ is the rms thermal velocity. $J_m$ and $I_n$ are the ordinary and modified Bessel functions, respectively, and $Z$ is the plasma dispersion function.[4] Space and time dependence is present through the potential which has the form $\phi(\mathbf{x},t)=\phi_0\exp(ik_x x+ik_z z-i\omega t)$. The electric field is given by $\mathbf{E}=-\nabla\phi$. What is important to note in Eq. (2) is that at a given point in space and time, the distribution function $f^1(v_y)$ contains information on $k_x$ and (obviously) on the field amplitude $\phi_0$. What may be less obvious is that, provided $|\zeta_n|>2$ for all $n$ (weak damping), there is only a weak dependence on $k_z$. For use later, we note that the Fourier transform on $v_y$ of (2) is given by

$$\bar{f}^1(K,\mathbf{x},t)=\frac{-q\phi(\mathbf{x},t)}{mv_t^2}\left[e^{-(Kv_t)^2/2}+\sum_{n=-\infty}^{\infty}\zeta_0 Z(\zeta_n)e^{-(\lambda+b^2)/2}I_n(\sqrt{\lambda}b)\right], \tag{3}$$

where $b\equiv\sqrt{\lambda}+Kv_t$. The summation in Eq. (3) is more quickly converging than that in (2), and is more easily generalized as well.

Equation (2) is related to the mobility[3] via

$$\langle v_y\rangle=M_{yx}E_x+M_{yz}E_z=\int_{-\infty}^{\infty}v_y f^1(v_y)\,dv_y, \tag{4}$$

where $\langle v_y\rangle$, the average dielectric velocity of the particle species in question, can be written

$$\langle v_y\rangle=(cE_x/B_0)M,\quad M=\sum_{n=-\infty}^{\infty}\zeta_0 Z(\zeta_n)\frac{d}{d\lambda}[I_n(\lambda)e^{-\lambda}]. \tag{5}$$

The function $M$ is simply related to the usual mobility via

$$M=(B_0/c)[M_{yx}+(k_z/k_x)M_{yz}].$$

For a propagating wave, the parameters in Eqs. (2), (3), and (5) will not be arbitrary, but will be constrained by the electrostatic dispersion relation

$$\epsilon=k_x^2+k_z^2+\sum_s k_{Ds}^2 \sum_{n=-\infty}^{\infty}[1+\zeta_{0s}Z(\zeta_{ns})]e^{-\lambda_s}I_n(\lambda_s)=0, \tag{6}$$

where $k_{Ds}^2\equiv 4\pi n_s q_s^2/m_s v_{ts}^2$ is the inverse Debye length squared. We have introduced a species label $s$, which is summed over the electron and ion species. Figure 1(a) shows the real part of $\epsilon$ as a function of $k_x v_{ti}/\Omega_{ci}=\sqrt{\lambda_i}$ for $\omega/\Omega_{ci}=2.75$ and $\zeta_{0i}=20$. In order of increasing $\lambda_i$, the two zeros correspond to the electrostatic ion-cyclotron wave (EICW) and the neutralized ion Bernstein wave (NIBW).[5] Figure 1(b) shows the normalized mobility $M$ for the same parameters as in Fig. 1(a) and indicates that there are currents transverse to both the EICW and the NIBW.

These formulas suggest that local phase-locked measurements of the distribution function, transverse to an electrostatic wave, carry information on the wave amplitude and on the wavelength perpendicular to the magnetic field. Because plasma dielectric response depends on the history of particle trajectories as they pass through the wave, information on the wave number is present.

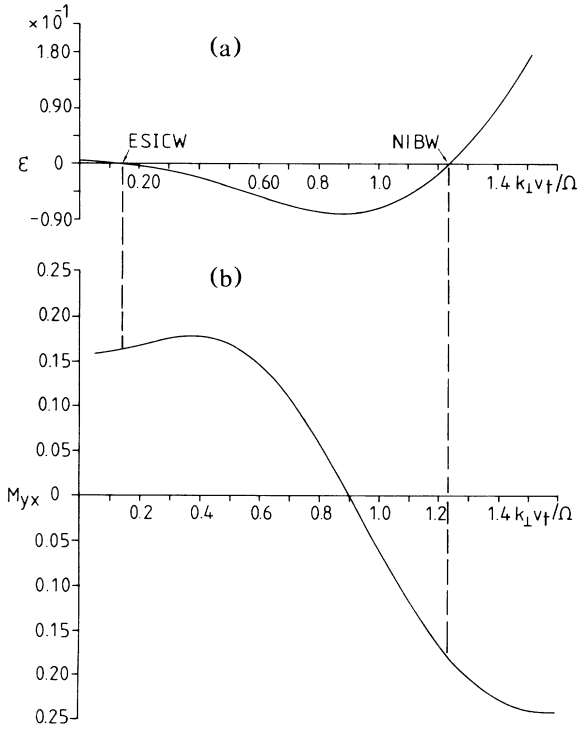


FIG. 1. (a) Electrostatic dielectric constant vs $k_x v_t/\Omega_{ci}$ for $\omega/\Omega_{ci}=2.75$. Zero crossings indicate propagating waves. (b) Transverse mobility indicates transverse currents in the presence of an electric field.

In order to test these predictions, neutralized ion Bernstein waves were generated in an argon discharge plasma with density $n_e\simeq 10^{11}$ cm$^{-3}$, temperatures $T_e\simeq 14$ eV, $T_i\simeq 0.1$ eV, and magnetic field $B_0=2$ kG. The cylindrical plasma has a radius of 2.5 cm and a length of 500 cm. Because the NIBW has a perpendicular phase velocity near the ion thermal speed, the perpendicular wavelength of the electric field is readily "detected" by the plasma ions.

Measurements of the ion-velocity distribution are made using laser-induced fluorescence.[1] A tunable pulsed dye laser is used to excite resonant transitions in the plasma (argon) ions (see Fig. 2). The measurement volume is localized to a cylindrical section ($\simeq 50$ mm$^3$), being defined by the intersection of the laser beam and the viewing volume of the detection system. By triggering the laser at a definite point in the wave phase, ion velocities coherent with the applied waves can be detected. Both the pulse duration (10 nsec) and triggering jitter ($<1$ $\mu$sec) are much shorter than the wave period ($>10$ $\mu$sec).

From the measured distribution functions, the perturbation due to the wave, the average velocity (first moment), and the ion thermal velocity (second moment)

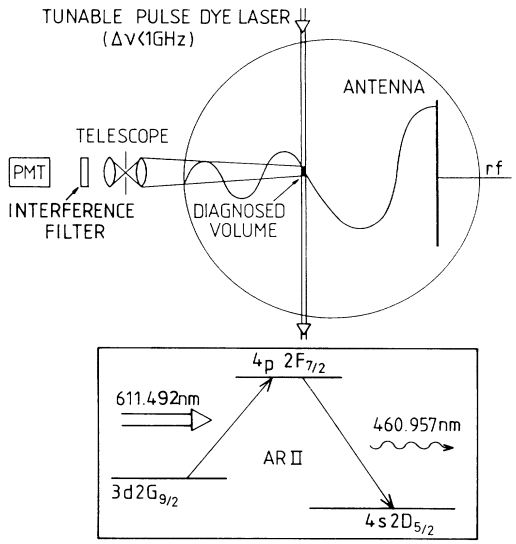


FIG. 2. Experimental setup and ionic transitions utilized.

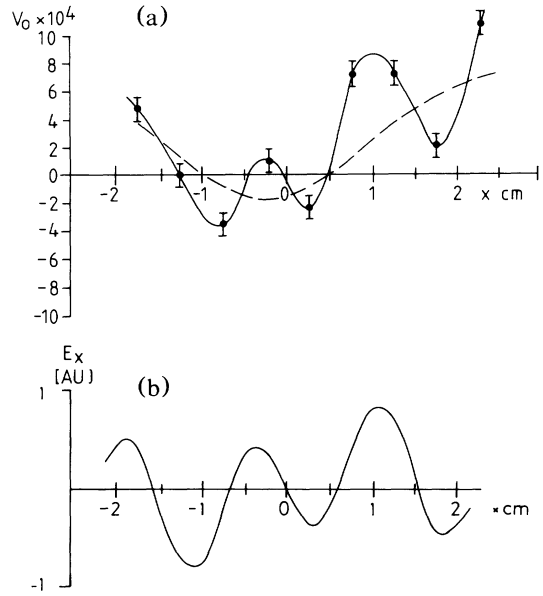


FIG. 3. (a) Snapshot of the average transverse ion velocity in the presence of waves. Solid curve is drawn through data points; dashed line indicates anticipated EICW wavelength. (b) Prediction of the wave form from the electrostatic wave equation; both the EICW and NIBW are included.

are obtained. Figure 3(a) shows a radial profile of the average transverse velocity when waves are generated at $\omega/\Omega_{ci}=2.75$. Figure 3(b) shows a prediction of the electric-field wave form starting from the electrostatic wave equation and the antenna structure (by a Fourier integral). Experimentally, the result is an interferogram of the wave electric field which the laser obtains without

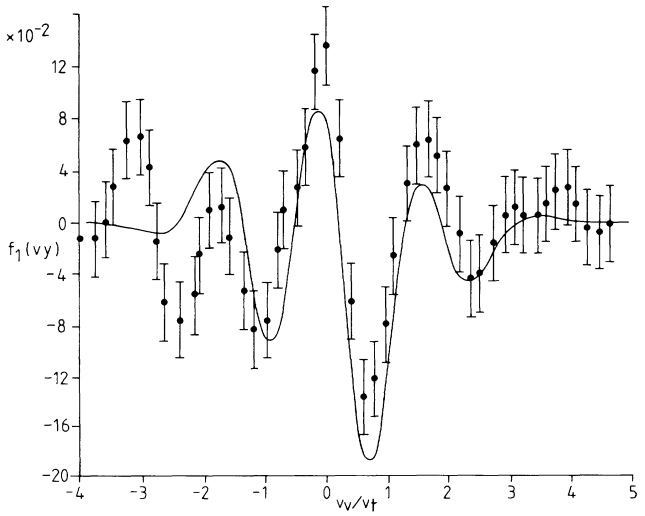


FIG. 4. Perturbed component of the ion distribution function. The solid curve is from Eq. (2) and the points are from laser data.

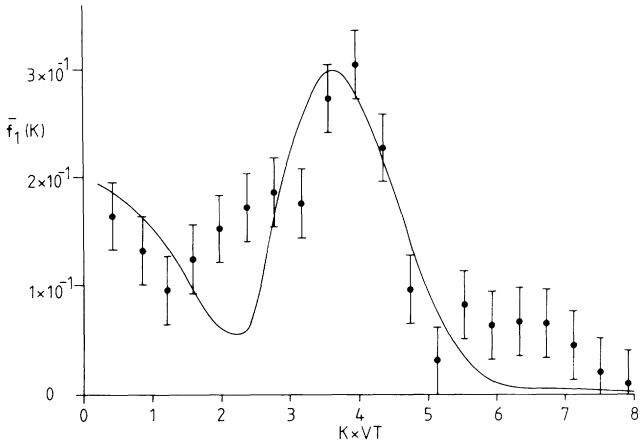


FIG. 5. Fourier transform of the perturbation. The solid curve is from Eq. (3) and the points are from laser data.

perturbing the plasma. Wavelengths similar to (or smaller than) the laser-beam size (4 mm in diameter), however, are not easily detected by this method. It should also be noted [cf. Fig. 1(b)] that the electric fields of the EICW and NIBW are detected with similar sensitivity but opposite sign.

The above procedure requires measurements of the average plasma response at several distinct locations. Figure 4 shows the perturbation of the ion distribution function (the unperturbed part has been subtracted) at a single point in space. The solid curve is the prediction of Eq. (2) [constrained by Eq. (6)] with $E_x c/B_0 v_t=0.6$. The EICW has a very subtle effect here (distortion of the base line) which tends to be masked by the NIBW. The oscillations indicate the value of $k_x$ (NIBW), and the amplitude of the perturbation ($\simeq 10\%$ here) indicates the electric-field amplitude $E_x$. In an alternative representation of the data, the Fourier-transformed perturbation [Eq. (4)] is compared, observing the usual precautions, with the discrete Fourier transform (DFT) of the data in Fig. 5. The prominence in the spectrum for $Kv_t \simeq 2k_x v_t/\Omega_{ci}$ is evidence of the modulation observed as a function of velocity in Fig. 4. Once again, the laser-beam diameter must be small compared with the wavelength of the plasma electric field for the measurement to be calibrated.

In the data presented here, the electric fields $E_x$ are on the order of a few volts per centimeter, indicating wave potentials of slightly less than a volt. The actual detection limit depends on the physical size and spectral width of the laser beam as well as the data-collection rate compared to the time over which the wave form is stable. In particular, a continuous-wave laser would probably be much better than a pulsed laser for these measurements. A further limitation is that, with increasing wave frequency $\omega/\Omega_{ci}$, the ion response is generally less important and, therefore, a larger electric field is necessary for

the same perturbation. We note that for electrostatic waves it is also possible to use a broadband laser (no velocity selection) to detect waves through oscillations in the ion density. The ability to measure plasma-wave electric fields without using probes which perturb the plasma can be very useful during experiments involving thresholds.[6] In addition to providing a demonstration of the linear dielectric response of the plasma ions, measurements of the perturbed distribution (Fig. 4) reveal the inherently kinetic nature of the NIBW. As a result of the distribution of ion velocities (which range both above and below the wave phase velocity), ion motion perpendicular to the magnetic field is responsible for both the inductive (positive-sign) and capacitive (negative-sign) components of the dielectric response which support the wave.

The authors would like to thank P. J. Paris for assistance with the experiments, R. A. Stern for helpful discussions, and M. Q. Tran for comments on the manuscript. This work is partially supported by the Swiss National Science Foundation under Grants No. 2.868-0.85 and No. 2.869-0.85.

[1]R. A. Stern, Bull. Am. Phys. Soc. **22**, 1122 (1977); R. A. Stern, D. N. Hill, and N. Rynn, Phys. Rev. Lett. **37**, 833 (1981).

[2]R. McWilliams and D. Sheehan, Phys. Rev. Lett. **56**, 2485 (1986).

[3]T. H. Stix, *The Theory of Plasma Waves* (McGraw-Hill, New York, 1962), p. 186.

[4]B. Fried and S. Conte, *The Plasma Dispersion Function* (Academic, New York, 1961).

[5]J. P. M. Schmidtt, Phys. Rev. Lett. **31**, 982 (1973).

[6]F. Skiff, F. Anderegg, and M. Q. Tran, Phys. Rev. Lett. **58**, 1430 (1987).